NASA Technical Memorandum 81770

Free Radical Propulsion Concept

C. E. Hawkins and S. Nakanishi
Lewis Research Center
Cleveland, Ohio

Prepared for the
Fifteenth International Electric Propulsion Conference
cosponsored by the American Institute of Aeronautics and Astronautics,
the Japan Society for Aeronautical and Space Sciences,
and Deutsche Gesselschaft fur Luft- und Raumfahrt
Las Vegas, Nevada, April 21-23, 1981

NASA

N81-20180

ERRATA

NASA Technical Memorandum 81770

FREE RADICAL PROPULSION CONCEPT

C. E. Hawkins and S. Nakanishi

April 1981

The attached pages 20, 21, and 22 should be inserted in the report at the end of appendix E.

FREE RADICAL PROPULSION CONCEPT

C. E. Hawkins and S. Nakanishi

National Aeronautics and Space Administration
Lewis Research Center
Cleveland, Ohio 44135

ABSTRACT

A free radical propulsion concept utilizing the recombination energy of dissociated low molecular weight gases to produce thrust is examined. The concept offers promise of a propulsion system operating at a theoretical impulse, with hydrogen, as high as 2200 seconds at high thrust to power ratio, thus filling the gap existing between chemical and electrostatic propulsion capabilities.

Microwave energy used to dissociate a continuously flowing gas is transferred to the propellant via three-body-recombination for conversion to propellant kinetic energy. In preliminary experiments, power absorption by the microwave plasma discharge was in excess of 90 percent over a broad range of pressures. Gas temperatures inferred from gas dynamic equations showed much higher temperatures from microwave heating than from electrothermal heating. Spectroscopic analysis appeared to corroborate the inferred temperatures of one of the gases tested.

E-813

INTRODUCTION

Studies have been performed to define the propulsion system requirements for various types of future space missions. In particular, the characteristics of chemical and electric propulsion for orbit raising missions can be compared by the methodology used in reference 1. Figure 1 shows the performance of chemical and electrostatic ion propulsion systems in terms of the ratio of total mass required in Low Earth Orbit (LEO) to payload mass in Geosynchronous Orbit (GEO) as a function of specific impulse (I_{sp}). The total mass in LEO is crucial because the earth-to-orbit cost is a major fraction of overall mission cost. Present chemical systems are limited to operation at I_{sp} less than about 500 seconds at which point the payload mass ratio is greater than three and rises very rapidly with decreasing specific impulse.

Electrostatic mercury ion thrusters operate efficiently at values of I_{sp} above 1800 seconds resulting in payload mass ratios from about 2.5 to 1.25 depending upon the trip time and specific impulse. Because of the low thrust characteristics, however, trip times with electrostatic ion thrusters are from about 50 to 250 days in contrast to chemical system trip times which may be less by one to two orders of magnitude. In general, chemical rockets produce high thrust at high thrust density (thrust per unit cross-sectional area) but at low specific impulse. Electrostatic ion thrusters, on the other hand, operate at high specific impulse but very low thrust and thrust density. A gap in performance characteristics exists between these two systems. Free radical propulsion has the potential of filling this gap.

The use of free radicals in rockets has been proposed previously with possible methods for storing the highly reactive propellants (ref. 2). Storage requirements, however, imposed considerable complexity and difficulty such as high magnetic fields, high pressures, or cryogenic systems.

The concept discussed in this paper differs from previous approaches in that no storage of free radicals is required. Electrical energy is used for a continuous-flow production of free radicals which are recombined to produce a high velocity propellant. The proposed concept is really a hybrid of chemical and electric propulsion in which electrically energized propellant is expanded through a nozzle to obtain high specific impulse at appreciable thrust levels. This paper first defines the basic concept of free radical propulsion and then presents results of both previous work and of recent experiments on various physical processes important to the concept.

Concept Summary

A schematic diagram of the free radical propulsion concept is given in figure 2 which shows the major physical processes to be discussed in more detail later. Electrical energy is converted to microwave energy which is applied to a candidate propellant. The microwaves create a plasma and the electromagnetic energy is absorbed primarily by the electrons. Energetic electrons dissociate the molecular propellant to form free radicals, atomic species, and ions. Table I shows some of these radicals of interest and their dissociation energies. If the dissociated radicals are recombined to regain the dissociation energy, one obtains the corresponding theoretical specific impulse values given in table I, assuming 100 percent energy conversion. A third body gas is added to enhance and to stabilize the volume recombination process and possibly to minimize wall recombination which results in wall heating losses. The recombined propellant is expanded through a nozzle to produce thrust.

Example System

To provide insight into the potential characteristics of free radical systems, a hypothetical 1-newton thruster using hydrogen propellant will be evaluated. A specific impulse of 1500 seconds will be assumed, which is considerably less than the theoretical limit of table I. The selection of thrust and specific impulse specifies a mass flow rate of 6.8×10^{-5} kg/sec. If it is assumed that all the power goes directly into dissociation and is subsequently converted ideally into kinetic energy of the propellant, the minimum input power required would be 7.3 kW. Using the I_{sp} and isentropic nozzle flow equations given in appendix A, the minimum flow area (nozzle throat) is 4×10^{-2} to 4×10^{-4} m^2 for stagnation pressures of 13.3 to 1330 newtons/m^2 (0.1 to 10 torr), respectively. These pressures were selected to span a range over which highy dissociated microwave discharges have been obtained and reported in the literature. With a typical expansion ratio of 25, the nozzle exit area will be of the order of 10^{-2} m^2, or an exit diameter of 11.5 cm for the higher pressure condition. High performance electrostatic ion thruster systems presently operate at specific impulses of about 3000 seconds at a power to thrust ratio of about 10 kW/newton. Thus, the free radical propulsion concept may theoretically operate at 1/3 to 1/2 the imput power, allowing for D.C. to microwave conversion and coupling losses.

The thrust density of electrostatic ion thrusters is typically 2 to 6 newtons/m^2. If the nozzle exit area of a free radical rocket is of the order of 10^{-2} m^2, the thrust density is almost two orders of magnitude greater than attainable with ion thrusters. The promise of increased thrust, thrust

density, and thrust to power ratio are features which lead to the interest in free radical propulsion.

Experimental Background

The successive physical processes inherent in the free radical propulsion concept are: (1) coupling or absorption of electromagnetic energy by electrons in the propellant system, (2) generation of free radicals, (3) transfer of the previously absorbed energy to the gas nuclei by recombination, momentum exchange, or other processes, and (4) conversion of the transferred energy into translational or gas kinetic energy accompanied by loss mechanisms. In a real microwve discharge, the first three processes occur simultaneously in an inseparable manner. The fourth process is one of converting random kinetic energy in a gas into directed energy. The thermodynamic process of gas expansion applied to chemical propulsion is also applied herein but will not be discussed at length.

For purposes of discussion, specific experimental results from the published literature and from recent experiments will be described, which have strong relevance to one or more of the above processes.

Power absorption. - Absorption of microwave power by a variety of gaseous media has been measured over a broad range of flow rates and pressures. Figure 3 shows the power absorption by argon in a cylindrical coaxial cavity at pressures less than 10 torr at a frequency of 460 MHz (ref. 3). The fraction of incident power absorbed reached 90 percent or higher over the pressure range tested. Similarly efficient absorption in argon of 2450 MHz power up to 1 kW, also with a cylindrical cavity, was reported in reference 4.

Power absorption by gases at higher pressures of 1×10^5 to 3×10^5 newtons/m^2 (760 to 2280 torr) has been studied (ref. 5). These pressures are orders of magnitude higher than those commonly used in gas dissociation studies and which were assumed for the example thruster. As the data will show, power absorption occurs even at elevated pressures, thus making this aspect of the free radical propulsion concept applicable to a broad range of operating conditions and mass flow, or thrust level.

Both pulsed waves and continuous waves at 3 gHz were applied in a tapered cylindrical wave guide containing the gas. Figure 4 shows the absorption characteristics in helium and argon gases. The pulses were typically 250 kW at pulse durations of 3 to 10 microseconds. Average incident power was 413 W. Better than 90 percent of the incident power was absorbed in helium, and considerably less power was absorbed in argon.

Continuous-wave experiments at discharge durations from 12 to 102 seconds obtained absorptions of 25 to 60 percent. The lower power absorption by argon in this experiment compared to that of reference 3 might be attributable to the wide differences in the methods used for coupling the microwave energy and in the test conditions.

The absorption of microwave power in helium and hydrogen using a resonant cavity has been investigated at the Lewis Research Center. Hydrogen is of particular interest as a candidate propellant because of its high recombination energy and low molecular weight.

The experimental apparatus described in appendix B permitted testing of a variety of gases over a range of flow rates, pressures, and input powers. At a given flow rate, absorption of microwave power by the gas was possible over a wide range of coupler location relative to the venturi throat. As seen in figure 5, the absorption was in excess of 95 percent except at very

small distances where it decreased. The coupler penetration and cavity length were adjusted for a particular resonant mode with optimum tuning at all times. At very short coupler-to-throat distances, the power absorption decreased, probably because the plasma volume decreased as it passed through the throat. The visible plasma extended, at most, about 3 cm past the throat into the region of rapidly decreasing pressure. Varying degrees of power absorption in other cavity resonance modes were also obtained. The maximum power absorption, however, was achieved in the mode used to obtain the data of figure 5 with minor adjustments to match changes in plasma conditions.

The above experimental evidences indicate that microwave power can be readily absorbed by a gaseous medium over a broad range of pressure and driving frequency. The power absorption process, therefore, is not expected to be a deterrent to the free radical propulsion concept.

Free radical generation. - Electrons with energies increased by the oscillating microwave electric field can undergo numerous collisions with gas molecules. The collision frequency is a function of the electron velocity, particle number density, and collision cross-section. Upon impact or interaction of electrons with other particles, one or more of the various possible phenomena such as momentum transfer, dissociation, excitation, or ionization may occur. The probabilities and energetics of these processes have major impacts upon the system parameters and requirements for a free radical propulsion system. Some of the experimental results reported in the literature on microwave plasma discharges will be reviewed in light of these system considerations.

Collisional processes in hydrogen have been widely investigated. In 1958, production of atomic hydrogen was investigated by passing a continuous stream of low-pressure hydrogen in a 1-cm diameter x 70-cm long quartz tube contained in a microwave resonator (ref. 6). An electron spin resonance spectrometer and recombination calorimeter were used to measure the number of atoms in the flowing gas. An optimum discharge pressure was observed above and below which the yield of atomic hydrogen decreased. The yield of hydrogen atoms reached a maximum at 66.7 newtons/m^2 (0.5 torr) but decreased about 25 percent at 33.3 newtons/m^2 (0.25 torr). At a flow rate of 2×10^{-6} kg/sec (10^{-5} moles/sec) and 66.7 newtons/m^2 pressure, with 100 W of 3000 MHz power absorbed in the discharge, the hydrogen gas was about 90 percent dissociated. At the same pressure and power level, when the flow rate was increased to 3×10^{-7} kg/sec, the absolute yield of atoms increased, but the fraction of dissociation decreased to about 25 percent.

From the optimum measured yield of hydrogen atoms and the power dissipated in the discharge, the energy efficiency was calculated to be 6.5×10^{-2} dissociations per electron volt, or 15.4 eV/dissociation. This is considerably higher than the theoretical hydrogen molecule dissociation energy of 4.477 eV (ref. 7). With allowances for measurement errors, the remainder of the dissipated energy was probably lost to wall recombination, and collisional processes such as electronic excitation.

In another study, up to 1500 W of microwave power at 2464 MHz was used in a resonant cavity with a quartz tube to produce free radicals of various gases (ref. 8). The free radical flux was measured by the linear portion of the time-temperature rise curve of a stainless steel block of known mass placed in the effluent stream. Over a pressure range of 2.1×10^3 to 2.7×10^4 newtons/m^2 (16 to 200 torr), the maximum yield of hydrogen atoms was 1 g atom/kW-hr, which converts to an energy efficiency of 74 eV/dissociation.

More recent studies into the energetics of gas dissociation in microwave discharges are being conducted at Michigan State University, and they are the subjects of companion papers at this conference (refs. 9 and 10).

Previous experiments described in the literature have reported high dissociation yields at energy costs considerably in excess of the dissociation or bond energy. It is not clear whether the dissociation process indeed requires this excess energy or repeated dissociation and recombination occur before a net yield of uncombined radicals is obtained. In the free radical propulsion concept, the objective is not a final yield of radicals but rather a high kinetic energy propellant exhaust. If the dissociation-recombination sequence can effectively transfer the absorbed microwave energy without major losses, the free radical propulsion concept may result in useful overall efficiencies regardless of measurable dissociation yield.

Energy transfer to gas molecules. - In microwave discharges, the energy is primarily absorbed in the electron gas. Electron temperatures are estimated to reach tens of thousands K. Some mechanism is required to transfer the absorbed energy to the gas molecules.

The transfer of energy by elastic collisions between electrons and the gas molecules is very inefficient. As shown in appendix C, the energy transfer is only a fraction of a percent under ideal conditions because of the large mass difference between the electrons and molecules.

Energy released upon recombination of dissociated atoms has promise of providing efficient energy transfer to the gas molecules. It is well known that a third body is necessary in atomic and radical recombination to stabilize the recombined molecule. The partitioning of energy upon recombination and the processes taking place in the conversion of large amounts of this released energy into translational, vibrational, rotational, or electronic energy are not clearly understood at present. Theoretical studies on recombination kinetics are being performed and will be discussed in a companion paper at this conference (ref. 11).

In the investigation of reference 8 an interesting observation was that although the temperature of the steel block placed in the effluent stream of dissociated hydrogen rose as much as 130° C, a point in the gas stream 4 cm downstream of the block rose only 6° to 8° C above the temperature of the inlet gas. The heat of recombination was, therefore, transferred to the block which functioned as a third body. The temperature rise of the block was not due to impact of a thermally hot gas stream.

Some properties of a nonequilibrium plasma can be seen in figure 6 (refs. 12 and 13). The electron temperature and gas temperature for an argon arc plasma at 1 atmosphere were measured spectroscopically. Even at this pressure and a neutral gas number density around 10^{18} cm^{-3}, the plasma was not in thermal equilibrium until enough power was delivered to raise the electron concentration above 10^{16} cm^{-3}. At lower pressures, the electron temperature was many times the gas temperature. The predilection to nonequilibrium plasmas at low pressures, however, does not preclude the formation of hot plasmas in a high frequency discharge. An induction-coupled torch flowing a mixture of argon and oxygen at 205 cm^3/sec and 47 cm^3/sec, respectively, at 1×10^5 newtons/m^2 (760 torr) pressure absorbed up to 3.08 kW of 4 MHz power (ref. 14). Measurements showed 1.14 kW of energy in the gas, 0.61 kW radiation losses, and 1.33 kW losses at the walls. Assuming local thermal equilibrium in the plasma, the maximum calculated gas temperature was 18 900 K at the axis. The average gas temperature integrated over the measured radial temperature distribution was 8500 K.

The energy balance indicated that losses at the wall exceeded the energy contained in the gas. Microwave discharge experiments usually require cooling of the containment vessel to avoid overheating. In quartz vessels which are widely used for these experiments, the heating is attributed to wall recombination of the discharge plasma and not dielectric heating by microwave absorption.

The mechanism by which absorbed microwave energy can be efficiently transferred to the gas molecules is not clearly evident. It is clear, however, that volume recombination must predominate over a wall recombination in order for the recombination process to be a useful mechanism of energy transfer. Wall site treatments such as recombination inhibitors or a buffer layer of molecular gas at the wall may provide an alternate third body for gas phase recombination and a transfer mechanism for the released energy.

Experimental Investigations

Preliminary experiments to examine the feasibility of energy transfer via the microwave dissociation-recombination cycle have been conducted using the apparatus described in appendix B. Gas temperature inferred from gas dynamics was selected as a means of evaluating the effectiveness of energy transfer. The inferred gas temperature which is related to the square of the pressure ratio between heated and unheated flow as developed in appendix D is shown in figure 7. The tests were performed with helium and hydrogen to compare the behavior of a nonatomic and a diatomic gas. The maximum inferred gas temperature, obtained with constant incident power, was affected by the axial distance of the coupler relative to the throat. The temperature obtained with helium was higher than with hydrogen, perhaps because the mass flow rates and the operating pressure ranges for the two gases were considerably different. For these tests, a fixed measured flow rate and a constant throat area made pressure and temperature functionally dependent.

A comparison of resistive and microwave discharge heating over a range of input power is shown in figure 8. The input power for the resistance wire heater was the product of the metered voltage and current to the heating element. The microwave input power was the absorbed power, or the difference between the incident and reflected powers. These tests were made to compare the relative effectiveness of energy transfer to the gas by electrothermal means and by the dissociation-recombination mechanism.

With resistive heating, the inferred gas temperatures were linear with input power as would be expected for constant mass flow rates and nearly constant specific heats of the gases. The input power to the resistive heater was limited to about 350 W to avoid heater failure. Even after allowing a long time for the gases to reach equilibrium, the gas temperatures did not exceed 700 K for helium and about 800 K for hydrogen.

The microwave heating of the gases was performed with the coupler-to-throat distance set at 6.4 and 4.5 cm for helium and hydrogen, respectively, corresponding to the peaks shown in figure 7. The output power from the microwave generator was adjustable between 300 and 600 W and the cavity was tuned for minimum reflected power at all times. With microwave heating, the inferred gas temperatures were about 1000 and 2000 K higher than with resistive heating at the same input power for hydrogen and helium, respectively. At approximately 600 W of input power, the inferred temperatures were 2800 and 3600 K for the two gases. From equation (A7) these gas temperatures would yield ideal gas specific impulses of 920 and 627 seconds for hydrogen and helium, respectively. The inferred temperatures obtained with helium,

which is a monatomic gas, were higher than with hydrogen. Gas flow rates and operating pressures were considerably different for the two gases in this test.

In a second series of tests with helium, hydrogen, and nitrogen, the flow rates were adjusted to give approximately the same operating pressure range for each gas. The coupler position, penetration depth, and cavity length were set at what appeared to be optimal for these pressures and returned as plasma conditions changed with input power.

The inferred gas temperatures obtained in the plasma discharge at approximately the same pressure for all three gases are shown in figure 9. Nitrogen was included to test a second diatomic gas and to provide a comparison with spectroscopic data to be discussed subsequently. Also included for comparison are the helium and hydrogen data from the earlier test (fig. 8). Comparison of the helium and hydrogen data obtained at approximately the same operating pressures shows that the inferred hydrogen temperature was rising rapidly with input power. The hydrogen test had to be terminated at an input power of about 350 W because the throat region of the venturi tube was incandescent and the pressure was rising steadily without reaching equilibrium.

Although not identical for all the gases, the operating pressure affected the inferred gas temperature significantly. A higher operating pressure level always tended to result in higher gas temperatures. Tuning characteristics, plasma luminosity, and wall heating were all different for different gases. These characteristics for any given gas also varied with pressure.

The inferred temperatures in nitrogen did not rise with input power as rapidly as in helium and hydrogen. The higher molecular weight and bond energy of nitrogen could be contributing factors to its temperature behavior. The temperature obtained from nitrogen spectroscopic data was in approximate agreement with the inferred temperature although the test conditions were considerably different, as described in appendix B.

The validity of these inferred gas temperatures is not certain. Furthermore, the exact mechanisms which lead to the high inferred gas temperatures are not clearly known. As indicated earlier, ionic and atomic recombination at the tube walls in both helium and hydrogen plasma discharges are thought to be responsible for heating the walls which were visibly and obviously hot. The softening point of fused quartz is approximately 1943 K. Because all parts of the venturi tube remained dimensionally intact, it could be concluded that even the hottest spot did not exceed softening temperature. Gas temperatures higher than 1943 K could not have been attained by convective heat transfer or surface accommodation as in resistive heating. Clearly, if the inferred gas temperatures are to be assumed correct, some form of energy transfer must be present in the microwave discharge. The gas flow rate was held constant and fully equilibrated with time. The observed rise in pressure indicates that the thermodynamic properties of the flowing gas were different between the heated and unheated cases. Detailed evaluation of these thermodynamic properties, possibly spectroscopically, and ultimately by direct measurement of jet thrust are required to determine the viability of the free radical propulsion concept.

In order to obtain a temperature measurement independent of the gas dynamic method, a spectroscopic method was implemented. This method uses measurements of the relative intensities of the rotational lines from a rotational-vibrational emission band of the molecular gas to obtain a rotational temperature, T_r.

The method therefore attempts to determine the average rotational kinetic energies of the gas molecules. If the rotational and translational motions are in equilibrium, this temperature is equivalent to the gas temperature, T_g. A discussion of the method and of the conditions under which $T_r = T_g$ is included in appendix E.

In a series of measurements on nitrogen, this method gave temperatures which rapidly increased with gas pressure, leveling off at $T_r = 2100$ K for $P_g = 10$ torr, as shown in figure 10. Attempts to run at higher gas pressures resulted in failure of the quartz flow tube.

These temperatures appear to support those obtained by the gas dynamics method. The latter gave $T = 1850$ to 2100 K at pressures of 14 to 16 torr and input powers of 300 to 600 W. The spectroscopic results gave $T = 1800$ to 2100 K at pressures of 5 to 10 torr. The input power was approximately 400 W. Spectroscopic measurements of hydrogen are currently being implemented.

CONCLUDING REMARKS

A free radical propulsion concept has been proposed. If successful, the concept will make available a high specific impulse propulsion system at thrust densities not currently attainable with ion propulsion.

A brief review of the published literature on high frequency discharges and preliminary experiments on a cavity-coupled microwave discharge in various gases have been performed. The absorption of incident power by the gaseous discharge was high in all cases, generally 90 percent or more.

The limited amount of available data on free radical generation does not permit a complete evaluation of the energetics or efficiency of this aspect of the free radical propulsion concept. High dissociation yield at energies considerably higher than the known dissociation energy has been obtained in a low pressure microwave discharge. Energy transfer to the propellant gas rather than the actual yield of dissociated species, however, may be more crucial to this propulsion concept.

Heating of the gas molecules by elastic collisions with energetic electrons is thought to be inefficient except possibly at high pressures and high power levels. The dissociation-recombination process involving third body molecular gas collisions is a possible mechanism for effective transfer of energy to gas molecules.

In preliminary experiments, diffusion of dissociated and ionized gases and recombination at the walls were predominant processes which limited tests to low pressures and power levels. Discharge gas temperatures inferred from gas dynamics considerations were as high as 3600 K. Temperatures derived from spectroscopic analysis of a nitrogen discharge were in substantial agreement with inferred gas temperatures. The direct measurement of jet thrust, correlation with measured temperatures, and evaluation of system energy efficiency need to be made before viability of the free radical propulsion concept can be firmly established.

APPENDIX A

PROPULSION FUNDAMENTALS

The equation for propulsive thrust is

$$F = \dot{m} V_e \tag{A1}$$

where

F thrust, N
$\dot{m}$ propellant mass flow rate, kg/sec
V_e exhaust velocity, m/sec

The ideal exhaust velocity of a gas after thermodynamic expansion is given by

$$V_e = \sqrt{2\,\Delta h} \tag{A2}$$

$$= \sqrt{2\,C_p(T_o - T)} \tag{A3}$$

where

h enthalpy, J/kg
C_p specific heat at constant pressure, J/(kg)(K)
T_o initial temperature, K
T final temperature, K

If the final temperature is assumed to be zero and the expansion is isentropic,

$$V_e = \sqrt{\frac{2k}{k-1} RT_o} \tag{A4}$$

where

k ratio of specific heats
R $\dfrac{\text{universal gas constant}}{\text{molecular weight}} = \dfrac{8314}{M} \left[\dfrac{J}{(kg)(K)}\right]$

By definition, the specific impulse, I_{SP}, is

$$I_{SP} = \frac{F}{\dot{m}g} \tag{A5}$$

where

g gravitational constant

If the exhaust gases are assumed to have a uniform velocity in the thrust direction,

$$I_{SP} = \frac{F}{\dot{m}g} = \frac{V_e}{g} \tag{A6}$$

Therefore, from equation (A4)

$$I_{SP} = \frac{\sqrt{\frac{2k}{k-1} \times \frac{8314}{M} \times T_o}}{g} \tag{A7}$$

$$= 24.6\sqrt{\frac{T_o}{M}} \text{ sec for diatomic gases, } k = 1.4$$

or

$$= 20.9\sqrt{\frac{T_o}{M}} \text{ sec for monatomic gases, } k = 1.66$$

If isentropic expansion of a perfect gas is assumed, the nozzle flow equation gives a minimum, or throat, area relation in the form

$$\frac{P_o A^*}{\dot{m}\sqrt{T_o}} = \left[\frac{k}{\left(\frac{8314}{M}\right)}\left(\frac{2}{k+1}\right)^{\frac{k+1}{k-1}}\right]^{-1/2} \tag{A8}$$

$$= 94.6\left[\frac{J}{(kg)(K)}\right]^{1/2} \quad \text{for} \quad M = 2 \text{ (hydrogen)}$$

or

$$= 62.9\left[\frac{J}{(kg)(K)}\right]^{1/2} \quad \text{for} \quad M = 4 \text{ (helium)}$$

where

P_o stagnation gas pressure, N/m^2
A^* minimum (throat) area, m^2
k ratio of specific heat
M molecular weight
m mass flow rate, kg/sec
T_o stagnation gas temperature, K

APPENDIX B

EXPERIMENTAL APPARATUS AND PROCEDURE

In order to gain insight into the behavior of microwave discharges and to obtain some indication of concept feasibility, preliminary experiments have been conducted at the Lewis Research Center. A schematic diagram of the experimental setup is shown in figure B-1. Microwave output power up to 600 W at 2.45 GHz from a magnetron generator was carried by a rectangular wave guide through a water cooled filter. The filter assured mode purity and also absorbed reflected power to protect the magnetron. A 40-dB directional coupler allowed measurement of incident and reflected power to a cylindrical resonant cavity. The cylindrical cavity was similar to that described in reference 4 and was 18.1 cm I.D. with water cooling coils brazed on the outer walls. A cooling air port forced an air jet normal to the cavity axis. A screened window allowed viewing and spectroscopic diagnostics.

The microwave power was coupled into the cavity by a coaxial rod terminated by a 1.9 mm diameter x 4 mm thick disk on the cavity end and a 17 mm diameter spherical knob on the waveguide-to-coaxial adapter end. The adapter was connected to the rigid directional coupler with a flexible waveguide. This allowed adjustment of the coupler penetration depth into the cavity for continuous optimum coupling of incident power.

The cavity length was also adjustable up to 14.2 cm to establish the desired resonant mode and to allow retuning as the plasma conditions changed. The retuning was possible under a wide range of plasma conditions because the ratio of plasma discharge tube diameter to cavity diameter was much less than unity. Thus the plasma only slightly perturbed the cavity resonance frequency.

Pressure-regulated gas from a storage cylinder passed through a flow meter. A variable leak valve controlled flow into the upstream end of a quartz discharge tube. Pressure within the discharge tube was measured by a multi-range capacitance-type gage with a resolution of 10^{-3} torr pressure. A flexible hose connected the exhaust end of the discharge tube to a vacuum facility through an adjustable valve.

Three types of quartz discharge tubes were used, two of which are shown in figure B-2. The first type (fig. B-2a, type 1) was a vacuum-jackated converging-diverging venturi tube fabricated of 25 mm I.D. fused quartz tubing. The downstream end of the vacuum jacket was an open annulus through which 0.05 mm thick stainless steel shim stock was inserted to provide a reflective radiation shield. This tube was used to evaluate gas heating by a nichrome wire resistive heating element.

The second type of discharge tube (fig. B-2b, type 2) was also a quartz venturi. The vacuum jacket was sealed at both ends and fitted with a 6 mm diameter tubing on the side. The side tubing was connected to a vacuum facility and pumped to approximately 10^{-5} torr. This vacuum jacket served three purposes: (1) provided a thermal barrier, (2) balanced the pressure across the hot venturi wall, and (3) permitted transmittance of the microwave without a gaseous breakdown in the vacuum jacket.

The third type of discharge tube was simply a 1.3 cm O.D. x 1.0 cm I.D. quartz tubing. The purpose of this experiment was to examine the gaseous discharge spectroscopically. The spectroscopic measurements were made with a 0.5 m focal length monochrometer having a spectral range of 2000 to 9100 angstroms with a resolution better than 0.5 angstrom.

Gas heating experiments were performed in the venturi tubes by using the resistance element heater or by applying microwave power upstream of the throat. The discharge pressure downstream of the throat was kept very low. At any given flow rate of gas, comparison of the upstream pressure with and without heating was used as an indication of the gas temperature as described in appendix D.

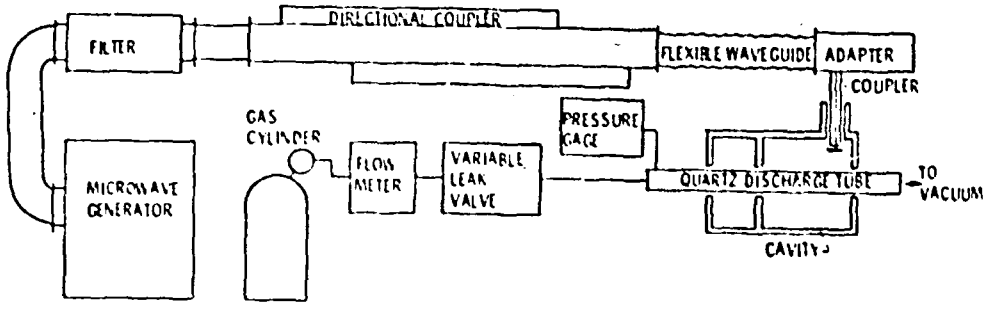

Figure B-1. - Schematic diagram of microwave discharge experiment.

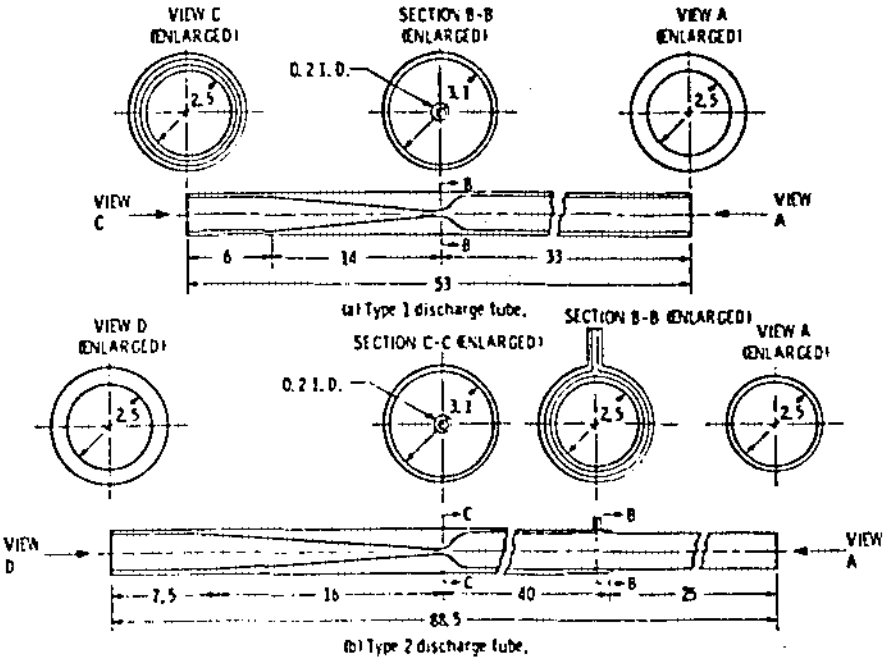

Figure B-2. - Schematic drawings and cross-sections of venturi discharge tubes. All dimensions in centimeters.

APPENDIX C

TRANSFER OF ENERGY BY ELASTIC COLLISIONS

The transfer of energy by elastic collision between a moving body of mass, m_1, and mass, m_2, at rest is given by

$$\frac{\Delta K}{K} = \frac{4\xi \cos^2 \phi}{(1 + \xi)^2} \tag{C1}$$

where

ΔK energy lost by m_1
K initial energy of m_1
ξ m_2/m_1
ϕ trajectory angle of m_2 after collision relative to initial direction of m_1

The maximum transfer of energy occurs in a head-on collision where $\phi = 0$. When the mass ratio, $\xi >> 1$ as in the case of an electron impacting a nucleus

$$\frac{\Delta K}{K} \rightarrow \frac{4}{\xi}$$

For a hydrogen nucleus

$$\xi = 3.6 \times 10^3 \quad \text{and} \quad \frac{\Delta K}{K} \approx 10^{-3}$$

APPENDIX D

INFERRED GAS TEMPERATURE

Consider the gas flow between two regions, ① and ②, connected by a small passage or aperture

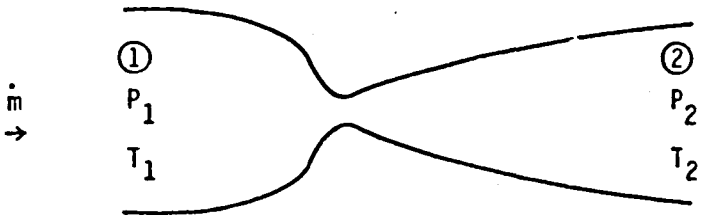

From appendix A, the mass flow rate under isentropic expansion is given by

$$\dot{m} = \frac{KP_1A^*}{\sqrt{T_1}} \tag{D1}$$

where

$\dot{m}$	mass flow rate
P	pressure
T	temperature
A*	minimum flow area
K	constant depending upon specific heat ratio and gas molecular weight

Free molecular effusion between two regions is given by (ref. 15)

$$\dot{m} = \frac{A^*(P_1 - P_2)}{\sqrt{2\pi RT}} \tag{D2}$$

where

R	gas constant

The assumption here is that the kinetic temperature, T, which determines free molecular velocity is equal in regions ① and ②. If a further assumption is made that $P_2 \ll P_1$, the equation reduces to

$$\dot{m} = \frac{A^*P_1}{\sqrt{2\pi RT}} \tag{D3}$$

which is the same form as equation (D1). Over the complete flow regime from free molecular to continuum flow, therefore, the inferred gas temperature upstream of the aperture or minimum flow area for the unheated and heated gases can be related to their corresponding pressures at a given mass flow rate, thus:

$$\frac{T_{1,\text{heated}}}{T_{1,\text{unheated}}} = \left(\frac{P_{1,\text{heated}}}{P_{1,\text{unheated}}}\right)^2 \qquad (D4)$$

APPENDIX E

SPECTROSCOPIC TEMPERATURE DETERMINATION

Spectroscopic methods of gas temperature determination (refs. 16 and 17) depend on the fact that in equilibrium, a collection of molecular oscillators is distributed among the available energy states, E_i, according to the Boltzmann factor $e^{-E_i/kT}$. Because the strength of a particular emission line is proportional to the number of molecules making the transition, one has

$$I_{em} \propto e^{-\Delta E_{ij}/kT} \tag{E1}$$

where ΔE_{ij} is the energy difference between the i and j states giving rise to the emission line of intensity I_{em}^{ij}.

In atomic spectroscopy, ΔE_{ij} is the energy difference between two electronic energy levels such as the Bohr levels of atomic hydrogen. For molecules, one must consider vibrational and rotational states of the molecule as a whole, in addition to the electronic energies. Electronic energies are typically of order 1 eV, vibrational energies of order 10^{-2} eV, and rotational energies of order 10^{-4} eV. The result is that each electronic transition gives rise to a group of vibrational bands, each of which consists of a series of closely spaced rotational lines. As a result of the close spacing of the rotational lines, instrumented response is not a major factor in determining relative intensities.

In a highly nonequilibrium situation, such as exists in a low pressure gas phase reaction system, one could have separate temperatures characterizing the average kinetic energy of each subsystem; for example, one could speak of vibrational temperature, rotational temperature, or gas temperature. One might expect that rotational and translational motions would reach a common equilibrium relatively quickly as a result of molecular collisions. That this is indeed the case is demonstrated by the work of Rudin (ref. 18) and Parker (ref. 19). The latter indicates that three to five collisions suffice to bring about rotational-translational equilibrium for common diatomic gases. In contrast, several thousand collisions are required to bring about vibrational-translational equilibrium.

In summary, the independence of relative intensities from instrumental response and the equivalence of rotational and gas temperatures combine to make rotational spectroscopy an attractive means of gas temperature determination.

The emission intensities of a single rotational band are given by

$$I_{em} = CS_J e^{-F(J)hc/kT_r} \tag{E2}$$

In this expression, C is a constant, S_J is a function of the rotational quantum number J, $F(J)$ is the energy difference in spectroscopic units, and the constants h, c, and k have their usual meanings. A plot of $n(I_{em}/S_J)$ versus $F(J)$ should give a straight line having a slope

$$m = -\frac{hc}{kT_r} \tag{E3}$$

Thus, a least squares fit of $\ell n(I_{em}/S_J)$ to $F(J)$ allows determination of T_r.

The nitrogen data were obained on the 0-2 vibrational band of the electronic transition known as the "second positive system" (ref. 20). This band consists of P-, Q-, and R-branches, due to different values of ΔJ, the change in the rotational quantum number. Useful data were obtained from the $J = 12$ through $J = 29$ lines of the R-branch, instrumental resolution being insufficient to separate the other lines. For each J value, there are three rib-bands in the R-branch, due to different values of the total angular momentum quantum number. In the R-branch of this band,

$$F(J) = B_2 J(J + 1) \tag{E4}$$

where $B_2 = 1.8149\ cm^{-1}$. Figure (E1) is a plot of $\ell n(I_{em}/S_J)$ versus $J(J + 1)$ for the R_1 and R_3 lines at a gas pressure of 5.0 torr. The plot for the R_2 line is essentially identical to the R_3 plot. As can be seen, the plots are not straight lines; in fact, they appear to be two intersecting straight lines. This is apparently due to self absorption (ref. 21). Based on the analysis in the above reference, we have used only the data for J values beyond the break in the curve to calculate temperatures. The values of T_r obtained for the R sub-bands give an indication of the precision of these temperature determinations.

Analysis of molecular hydrogen is in principle similar, but is complicated by the existence of few rotational lines in a given band and by a complex dependence of $F(J)$ on J. The 0-0 and 1-2 bands of the $3d'\Sigma_g \rightarrow 2p'\Sigma_u$ and the 1-2 band of the $3d'\pi_b \rightarrow 2p'\Sigma_u$ have been observed to date (ref. 22). Data are as yet insufficient to give reliable spectroscopic temperatures for hydrogen.

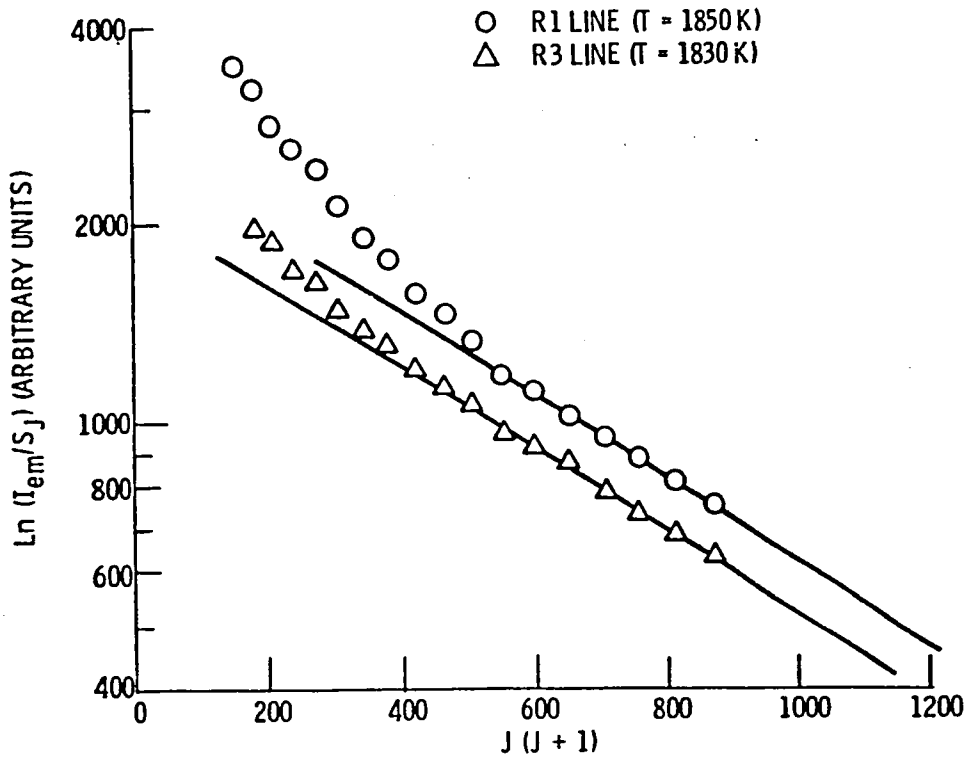

Figure E-1. - Emitted intensity of nitrogen rotational lines. Pressure 665 N/m^2 (5.0 torr).

REFERENCES

1. Byers, D. C., "Upper Stages Utilizing Electric Propulsion," NASA TM-81412, 1980.
2. Bass, A. M. and Broida, H. P., Formation and Trapping of Free Radicals, Academic Press, New York, 1960.
3. Moisan, M., Beaudry, C., and LePrince, P.; "A Small Microwave Plasma Source for Long Column Production Without Magnetic Field," IEEE Trans. on Plasma Science, Vol. PS-3, No. 2, June 1975, pp. 55-59.
4. Mallavarpu, J., Asmussen, J., and Hawley, M. C., "Behavior of a Microwave Cavity Discharge over a Wide Range of Pressures and Flow Rates," IEEE Trans. on Plasma Science, Vol. PS-6, No. 4, Dec. 1978, pp. 341-354.
5. Moriarty, J. J. and Brown, W. C., " Toroidal Microwave Discharge Heating of Gas," Journal of Microwave Power, Vol. 3, No. 4, Dec. 1968, pp. 180-186.
6. Shaw, T. M., "Dissociation of Hydrogen in a Microwave Discharge," Journal of Chemical Physics, Vol. 30, No. 5, May 1959, pp. 1366-1367.
7. Gaydon, A. G., Dissociation Energies and Spectra of Diatomic Molecules, 3rd ed., Chapman and Hall, London, 1968.
8. McCarthy, R. L., "Chemical Synthesis from Free Radicals Produced in Microwave Fields," Journal of Chemical Physics, Vol. 22, No. 8, Aug. 1954, pp. 1360-1365.
9. Brake, M., Hinkle, J., Wareck, J., Asmussen, J., Kerber, R., and Hawley, M., "Microwave Discharge Oxygen Plasmas," AIAA Paper 81-0674, Apr. 1981.
10. Hawley, M., Chapman, R., Filpus, J., Morin, T., Asmussen, J., Snellenberger, R., and Kerber, R., "Microwave Plasmas Generation of Hydrogen Atoms for rocket Propulsion," AIAA Paper 81-0675, Apr. 1981.
11. Etters, R. D. and Flurchick, K., "Atomic Hydrogen Rocket Engine," AIAA Paper 81-0677, Apr. 1981.
12. Okress, E. C., ed., Microwave Power Engineering, Vol. 2, Academic Press, New York, 1968.
13. Kolesnikov, V. N., "Arc Discharge in Inert Gases," Trudy Fizickeskoga Instituta, Akademiya Nauk SSSR, Vol. 30, 1964, pp. 66-157. Also in Physical Optics, edited by D. V. Skobel'tsyn, Transl. of Fizickeskaia Optika, Moscow, Izdatel'stvo Nauka, 1965, Plenum Publishing Corp., New York, 1966, pp. 53-123.
14. Reed, T. B., "Induction-Coupled Plasma Torch," Journal of Applied Physics, Vol. 32, No. 5, May 1961, pp. 821-824.
15. Dushman, S., Scientific Foundations of Vacuum Technique, John Wiley Sons, Inc., New York, 1949.
16. Herzberg, G., Spectra of Diatomic Molecules, Van Norstrand, New York, 1950, p. 124ff and p. 204ff.
17. Penner, S. S., Quantitative Molecular Spectroscopy and Gas Emissivities, Addison-Wesley, Reading, Mass., 1959, Ch. 17, pp. 475-531.
18. Rudin, M., "Criteria for Thermodynamic Equilibrium in Gas Flow," Physics of Fluids, Vol. 1, No. 5, Sep.-Oct. 1958, pp. 384-392.
19. Parker, J. G., "Rotational and Vibrational Relaxation in Diatomic Gases," Physics of Fluids, Vol. 2, No. 4, July-Aug. 1959, pp. 449-462.
20. Herzberg, G., Op. Cit., p. 271.
21. Penner, S. S., Op. Cit., p. 483ff.
22. Dieke, G. H., "The Molecular Spectrum of Hydrogen and its Isotopes," Journal of Molecular Spectroscopy, Vol. 2, No. 5, Oct. 1958, pp. 494-517.

TABLE I. – CHARACTERISTICS OF PROPELLANTS

Propellant radical	Molecular weight	Dissociation energy, J/kg	Theoretical specific impulse, sec (100 percent conversion)
H	1	217.8×10^6	2120
CH	13	45.6×10^6	1010
N	14	33.4×10^6	840
BH	12	25.9×10^6	734
NH	15	21.7×10^6	655
O	16	15.5×10^6	565

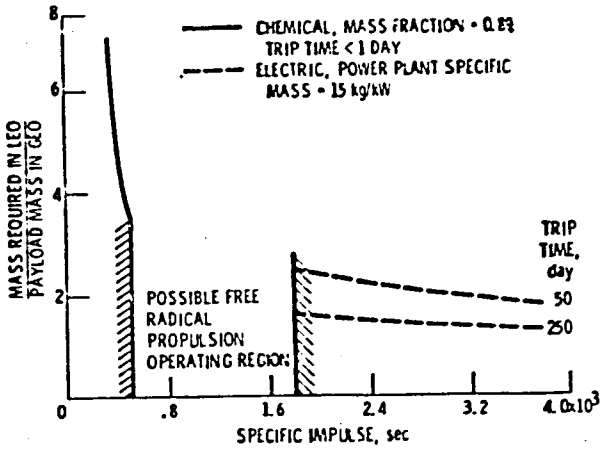

Figure 1. - Mass ratio of various leo to geo propulsion systems.

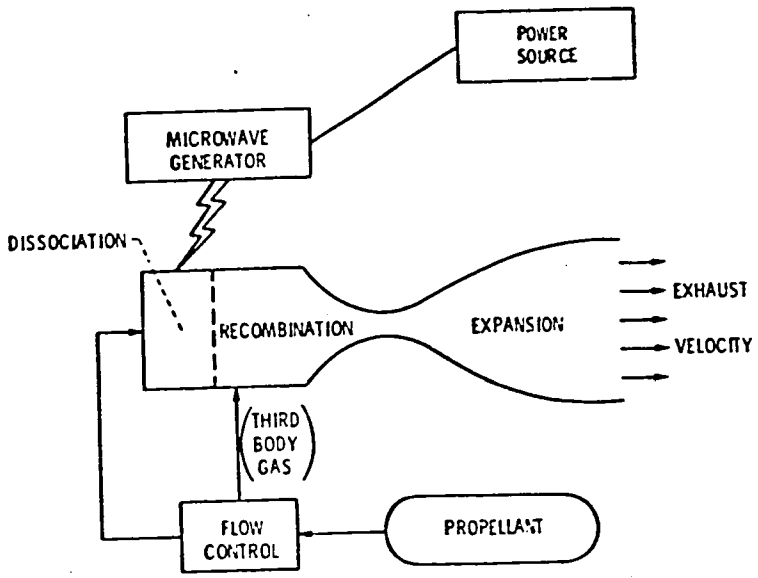

Figure 2. - Free radical propulsion concept.

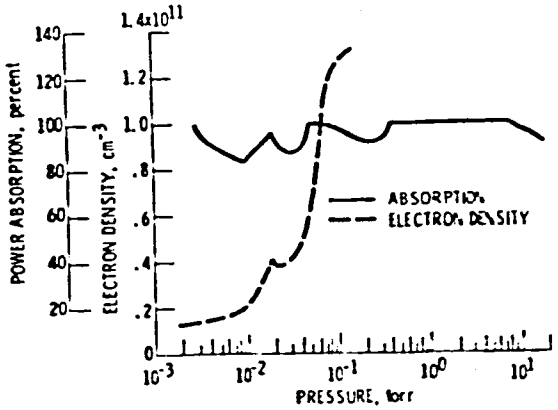

Figure 3. - Power absorption and electron density of an argon plasma discharge. Frequency, 460 MHz, incident power, 40 watt (ref. 3).

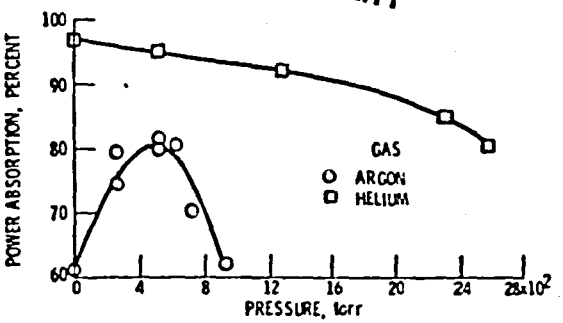

Figure 4. - Microwave absorption in gases. Frequency, 3000 MHz; average incident power, 413 watt (ref. 5).

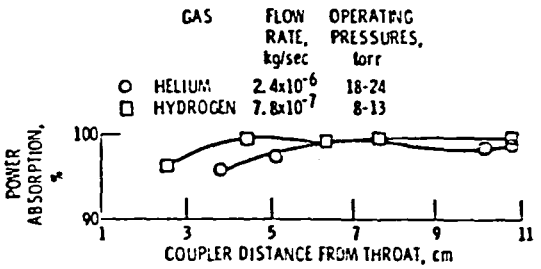

Figure 5. - Effect of coupler position on power absorption. Frequency, 2450 MHz; incident power, 300 W.

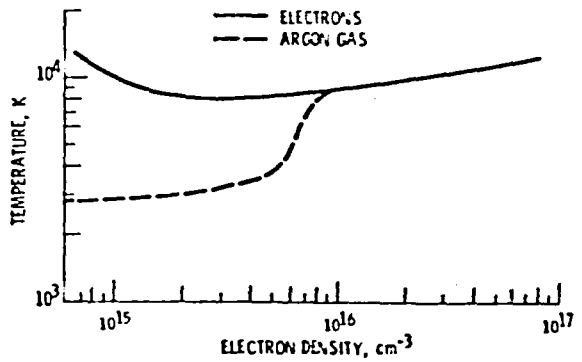

Figure 6. - Variation of temperature in an arc discharge at 750 torr pressure (refs. 12 and 13).

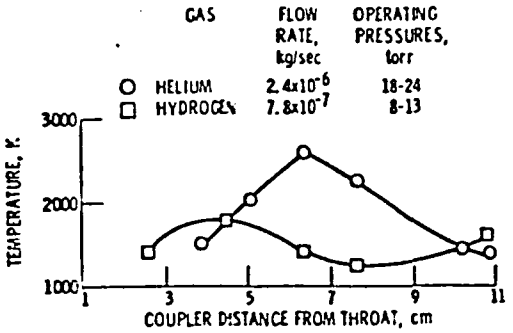

Figure 7. - Effect of coupler position on inferred gas temperatures. Frequency, 2450 MHz; incident power, 300 W.

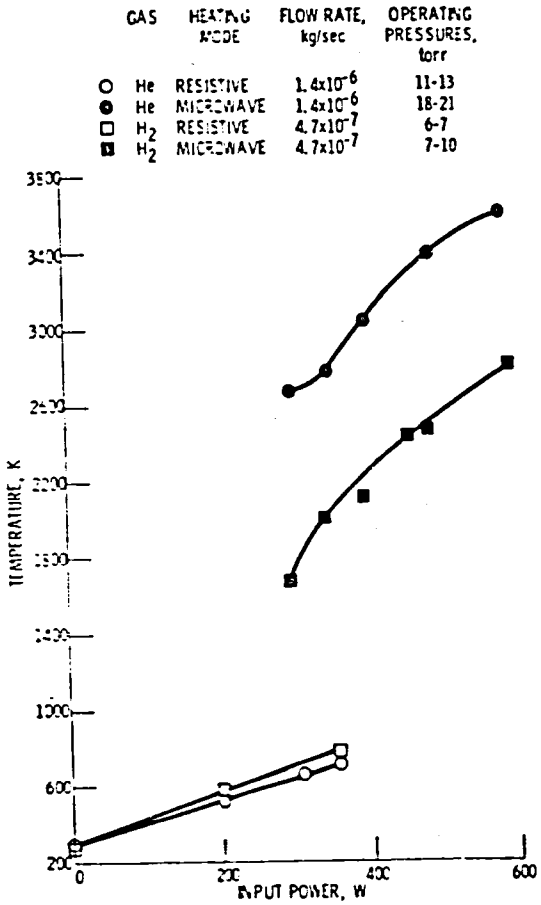

Figure 8. - Inferred gas temperatures obtained with resistive and microwave heating.

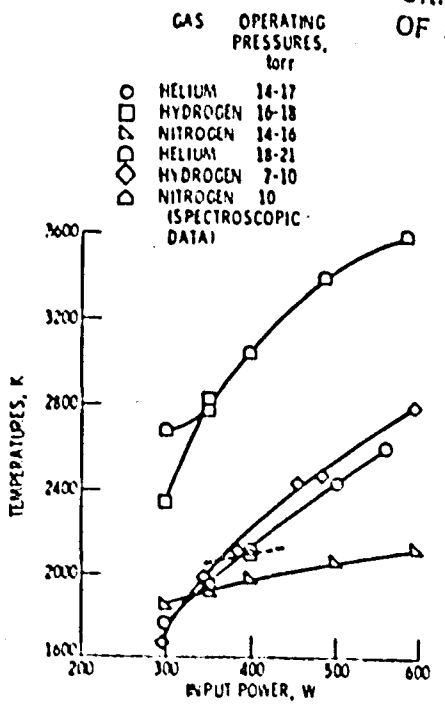

Figure 9. - Inferred gas temperatures of various gases in a microwave discharge.

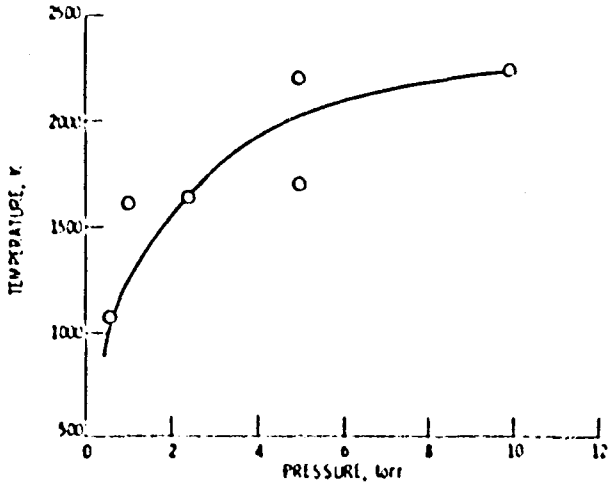

Figure 10. - Nitrogen discharge temperature from spectroscopic data R_1 lines only.